Paper No.
2381

NACE INTERNATIONAL CORROSION 2013 CONFERENCE & EXPO

# Corrosion Behavior of Deep Water Oil Production Tubing Material under Supercritical $CO_2$ Environment: Part II. Effect of Crude Oil and Flow

Fernando Farelas, Yoon-Seok Choi, Srdjan Nesic
Institute for Corrosion and Multiphase Technology,
Department of Chemical and Biomolecular Engineering,
Ohio University
Athens OH 45701
USA

Alvaro Augusto O. Magalhães, Cynthia de Azevedo Andrade
Petrobras
Rio de Janeiro, RJ 21941-915
Brazil

## ABSTRACT

Deep water oil production tubing materials are exposed to high $CO_2$ pressure and temperature conditions that can affect the corrosion performance of such materials. The present study aimed to evaluate the corrosion behavior of carbon steel exposed to supercritical $CO_2$/oil/brine mixtures at different water cuts (0, 30, 50, 70, and 100%), $CO_2$ partial pressures (8 and 12 MPa) and temperatures (65 and 90°C) in a flowing 25 wt.% NaCl solution. Corrosion behavior of carbon steel was evaluated by using electrical resistance (ER) measurements, weight loss measurements and surface analytical techniques (SEM and EDS). The corrosion rates of carbon steel increased with increasing water cut. There was no indication of corrosion attack with 0% water cut. At lower water cuts (30 and 50%), the steel surface was covered by iron carbonate ($FeCO_3$), while iron carbide ($Fe_3C$) was present on the steel surface at higher water cuts (70 and 100%) with very high corrosion rates. In addition, the presence of flow prevented the formation of protective $FeCO_3$ at high water cut conditions.

Keywords: Supercritical $CO_2$, carbon steel, water cut, crude oil, $CO_2$ corrosion, $FeCO_3$

## INTRODUCTION

Deep water oil production tubing materials usually are exposed to high $CO_2$ pressure and temperature conditions that can affect the corrosion performance of such materials. At temperatures above 31.1 $^oC$ and pressures higher than 7.38 MPa $CO_2$ is in its supercritical state. In the absence of water supercritical $CO_2$ is not corrosive, however under normal oil production operations produced water is always present. When $CO_2$ dissolves in water carbonic acid is formed ($H_2CO_3$) which significantly increases the corrosion rate of carbon steels. The mechanisms of $CO_2$ corrosion under supercritical conditions do not change compared to those identified at lower partial pressure.[1] An increase in the $CO_2$ partial pressure usually results in a drastic increase in the corrosion rate, behavior that is enhanced with temperature and flow.[2, 3]

In corrosion behavior of deep water oil production tubing materials in addition to the general factors ($CO_2$ partial pressure, temperature and flow), another important parameter has to be taken into account: the presence of crude oil. Carew *et al*.,[4] studied the effect of water cut, $CO_2$ and $H_2S$ partial pressures, temperature and flow velocity on the corrosion rate of API 5L[(1)] L80 steel. A mixture of 80% $CO_2$: 20% $H_2S$ was injected to the system and the pressure was increased up to ~20 MPa with nitrogen. The corrosion increased with water cut and no significant corrosion attack occurred at water cuts between 30% and 40%, however, general and localized attack was observed at water cuts greater than 40%. It was also reported that an increase in the rotational speed from 1000 to 4000 did not have a significant effect on the corrosion rate.[4, 5] The effect of supercritical $CO_2$ in multiphase flow using different pipeline steels has been also investigated.[6] It was reported that the corrosion rate increased with the water cut and below 50% water cut, the mixture was in the water-in-oil state. However, at water cuts greater than 50% the mixture switched to oil-in-water resulting in high general corrosion rate and pitting corrosion. Although studies on the general aqueous $CO_2$ corrosion in oil/water mixtures have been carried out and reported, there are no comprehensive studies available for crude oil/$CO_2$/brine environments at supercritical $CO_2$ condition.

The overall objective of the study was to evaluate the corrosion behavior of carbon steel in crude oil/supercritical $CO_2$/brine mixtures related to the deep water oil production development. In the part 1 of this study,[9] the corrosion properties of carbon steel were evaluated under different $CO_2$ partial pressures (4, 8 and 12 MPa) and temperatures (65 and 90$^oC$) in a 25 wt.% NaCl aqueous solution. In this part 2 of the same study the aim was to evaluate the corrosion behavior of carbon steel exposed to crude oil/supercritical $CO_2$/brine mixtures at different water cuts (0, 30, 50, 70, and 100%) in a flowing 25 wt.% NaCl solution.

## EXPERIMENTAL PROCEDURE

The corrosion experiments were carried out in a 4-liter stainless steel autoclave. A picture of the autoclave and experimental set up is shown in Figure 1. 28 API[(1)] crude oil was used in these experiments and water cut was varied from 0 to 100% with a 25 wt.% NaCl solution.

[(1)] American Petroleum Institute (API), 1220 L St. NW, Washington, DC 20005.

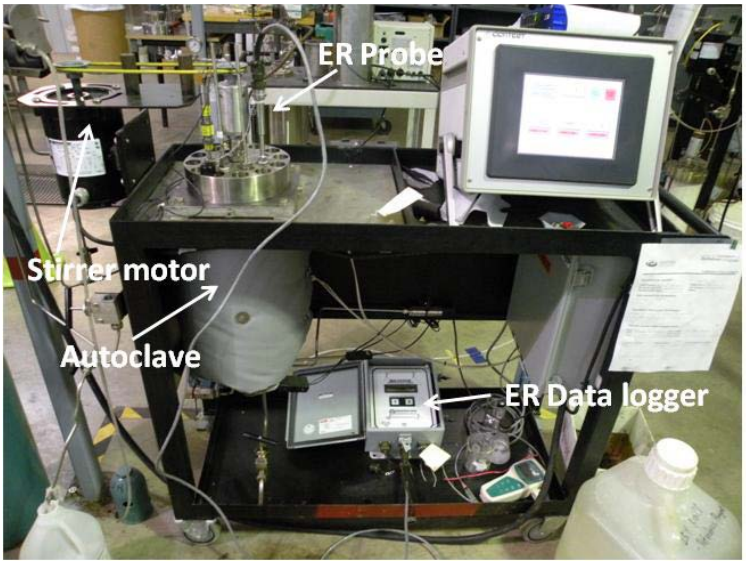


**Figure 1: Experimental Setup for Corrosion Test under High Pressure/Temperature Conditions and Different Water Cuts**

Table 1 shows the test matrix for corrosion testing. The experimental parameters were chosen based on the results obtained in part 1 of this study,[9] where localized corrosion was observed.

**Table 1**
**Test Matrix for Corrosion Testing**

| $CO_2$ pressure (MPa) | $CO_2$ phase | Temperature (°C) | Water cut (%) | Rotation speed (rpm) | Time (h) | Measurement techniques | Surface analysis |
|---|---|---|---|---|---|---|---|
| 8 | Supercritical | 90 | 0, 30, 50, 70, 100 | 1000 | 48 | Electrical resistance (ER) and weight loss | SEM, EDS, IFM |
| 12 | | 65 | | | | | |

Experimental procedure is as follows. Depending on the water cut selected for the test (Table 1), crude oil and 25 wt.% NaCl aqueous solution were placed together in a beaker and stirred overnight in order to form an emulsion. Then, the emulsion was transferred to the autoclave and deoxygenated with $CO_2$ for 1 to 3 hours. Meanwhile, two-square type API 5L L80 carbon steel samples (1.27 cm × 1.27 cm × 0.254 cm), with the chemical composition shown in Table 2 were ground with 600-grit silicon carbide paper, cleaned with isopropyl alcohol in an ultrasonic bath, and dried. Subsequently, an electrical resistance (ER) probe and the steel specimens were placed into the autoclave.

**Table 2**
**Element Analysis by Atomic Emission Spectroscopy for the Carbon Steel (API 5L L80) used in the Tests (wt.%)**

| C | Cr | Mn | P | S | Si | Fe |
|---|---|---|---|---|---|---|
| 0.30 | 0.85 | 0.91 | 0.015 | 0.008 | 0.29 | Balance |

The ER probe element was machined from the same material as the weight loss samples. The element is a wire loop with 2.03 mm thickness and a useful life of 0.5 mm. In ER measurement, the reduction in

cross-sectional area of an element of metal as it corrodes is accompanied by a corresponding increase in the electrical resistance (R) of the element. The relationship is given by Equation (1):[7]

$$R = r \times \frac{L}{A} \quad (1)$$

where L is the carbon steel element length, A is the cross sectional area, and r is the specific resistance. The probe reading represents the percentage of the effective probe element thickness consumed since the probe was inserted into the corrosive system. This value is most commonly used to calculate metal loss and/or corrosion rate, as shown below (Equations 2 and 3): [7]

$$ML = \frac{X \times K}{1000} \quad (2)$$

$$CR = \frac{(X_2 - X_1) \times K \times 365}{1000 \times T} \quad (3)$$

ML= metal loss in mils, X= instrument reading at any given time,
K= probe constant (=20), $X_2$= instrument reading at time $T_2$,
$X_1$= instrument reading at time $T_1$, T= time lapse (days) between readings $X_1$ and $X_2$,
CR= corrosion rate (mpy)

After closing the autoclave, an impeller was used to stir the emulsion at a rotation speed of 1000 rpm, stirring was maintained during the test (48 hours). Temperature was increased to the testing temperature and high pressure $CO_2$ was injected with a booster pump. After each test, the specimens were removed from the autoclave, rinsed with toluene, acetone, deionized water and isopropyl alcohol, dried with $N_2$ and stored in a desiccator cabinet for surface analysis (SEM, EDS).

## RESULTS AND DISCUSSION

### Experimental Study of Corrosion in $CO_2$/Oil/Water Environments

#### Experiments at 8 MPa and 90°C

Figure 2 shows the variation of metal loss with time obtained from ER measurements with different water cuts at 8 MPa and 90°C. The water cut was varied from 30 to 100%. The metal loss with 30 and 50% water cuts were quite similar and constant during the 48 hour of exposure. With 70% water cut, the initial metal loss was higher than that seen at lower water cut cases and slightly increased with time. Without the oil phase (100% water cut), the initial metal loss was much higher compared to lower water cuts and kept increasing during the 48 hour of exposure.

Figure 3 compares the average corrosion rate obtained from ER and weight loss measurements under different water cuts. As can be observed from Figure 3, the corrosion rate increased considerably with the increase of water cut. The corrosion rate slightly increased by increasing water cut from 30% to 50%, whereas it increased more than 4 times from 50% to 70% water cut. It can be assumed that the oil and water mixture was in its water-in-oil state below 50% of water cut, whereas the mixture was changed to oil-in-water state at higher water cuts.[6] However, it is important to note that even at low water cuts (30% and 50%), the corrosion rate was not negligible (e.g., 1.1 mm/y at 30% water cut and 3.4 mm/y at 50% water cut). Figure 3 also shows that the corrosion rates from both ER and weight loss measurements showed the same trend with different water cuts. However, there is a significant difference in corrosion rate between ER and weight loss measurements at 100% water cut and it can

be attributed to the presence of conductive layers which can affect the ER measurements.[8] In part 1 of this study,[9] the presence of iron carbide ($Fe_3C$) on the steel surface was detected by XRD analysis. $Fe_3C$ is an electrical conductor[10] and its presence will increase the apparent cross sectional area of the ER element and decrease the element's electrical resistance (see equation 1), which results in lowering of the corrosion rate reading, as is observed in Figure 3.

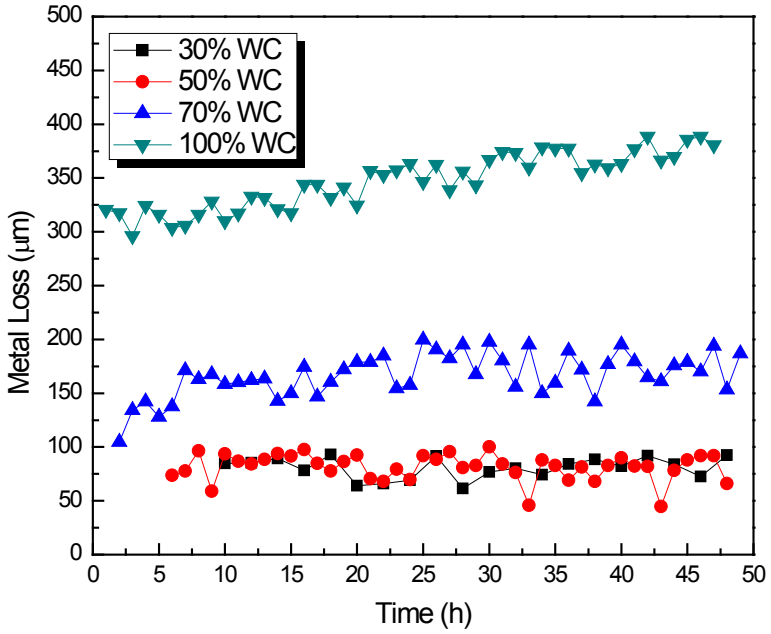


**Figure 2: Variation of Metal Loss with Time Obtained from ER Measurement at Different Water Cuts (8 MPa $CO_2$, 90°C, 1000 rpm)**

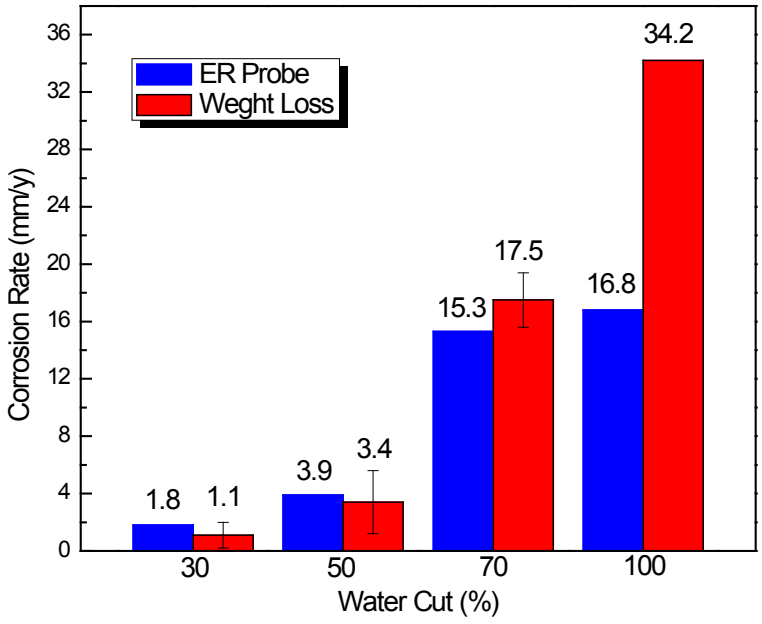


**Figure 3: Comparison of Corrosion Rates Obtained from ER and Weight Loss Measurements (average) with Different Water Cuts at 48 Hours (8 MPa $CO_2$, 90°C, 1000 rpm)**

The SEM surface observations and EDS analyses of the samples exposed to different water cuts are shown in Figure 4. Note that the morphologies were almost identical for 30% and 50% water cuts and

the EDS analysis of the surface suggested that it was covered predominantly by $FeCO_3$ (Figure 4a and Figure 4b).

For 70% and 100% water cut conditions, the steel surface appears to be much more severely attacked state. EDS analysis suggested that the corrosion product consists mainly of $Fe_3C$ with minor constituents of alloying elements from carbon steel. Although some $FeCO_3$ was found on the surface at 70% water cut (Figure 4c), it did not offer any protection against corrosion under this condition.

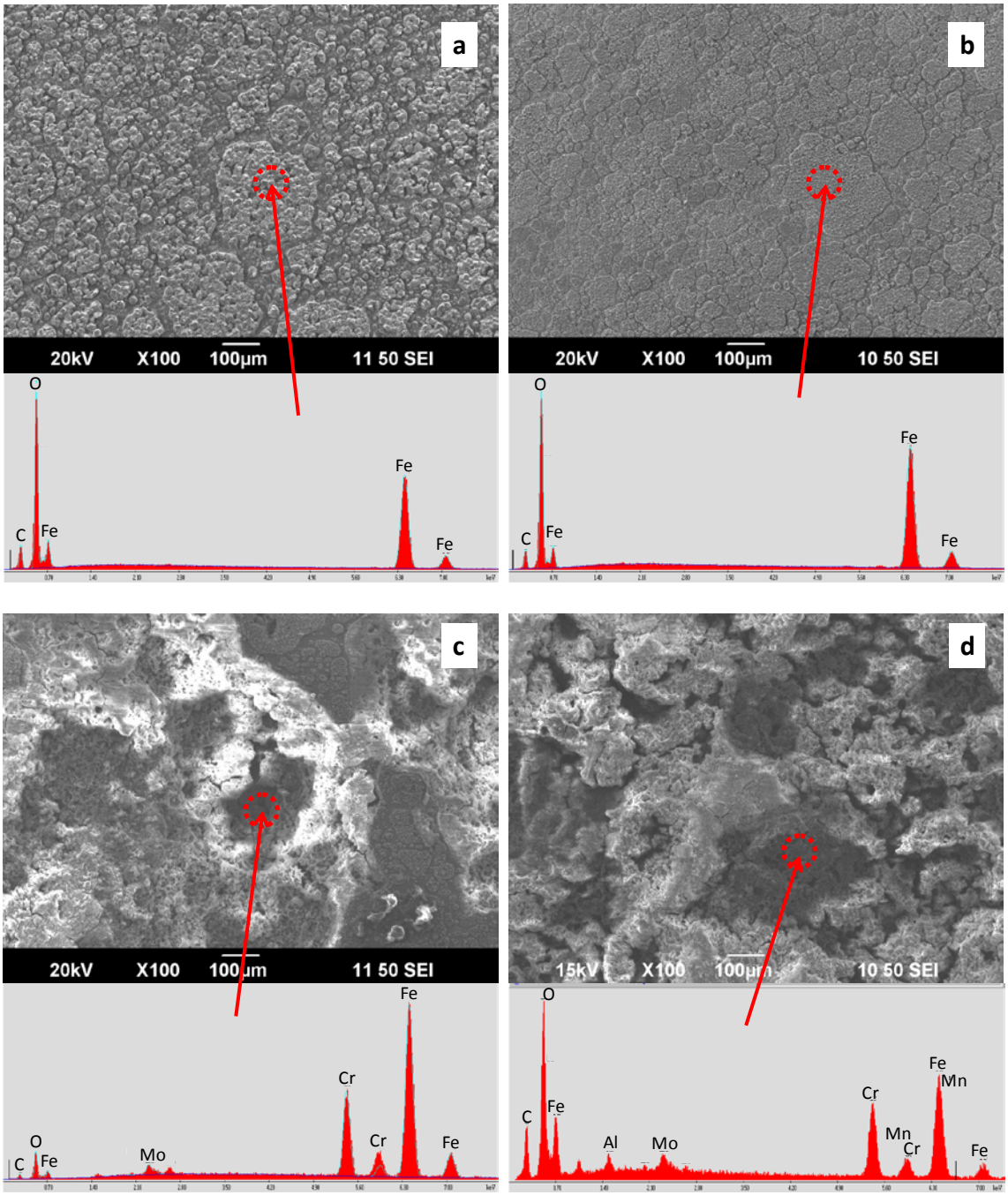


**Figure 4: SEM Images and EDS Spectra of the Corroded Surface of the Sample Exposed to: (a) 30%, (b) 50%, (c) 70% and (d) 100% Water Cut (8 MPa, 90°C, 48 hours,1000 rpm)**

Figure 5 shows the surface morphologies of samples after removing the corrosion product layer with Clarke solution.[11] At 30% and 50% water cut conditions, the original polishing marks were still visible on a fraction of the surface suggesting that it did not corrode much. A non-uniform corrosion attack can be observed at 30% and 50% water cut conditions. On the other hand, a severe uniform corrosion attack was observed on the surface for samples at 70% and 100% water cut conditions.

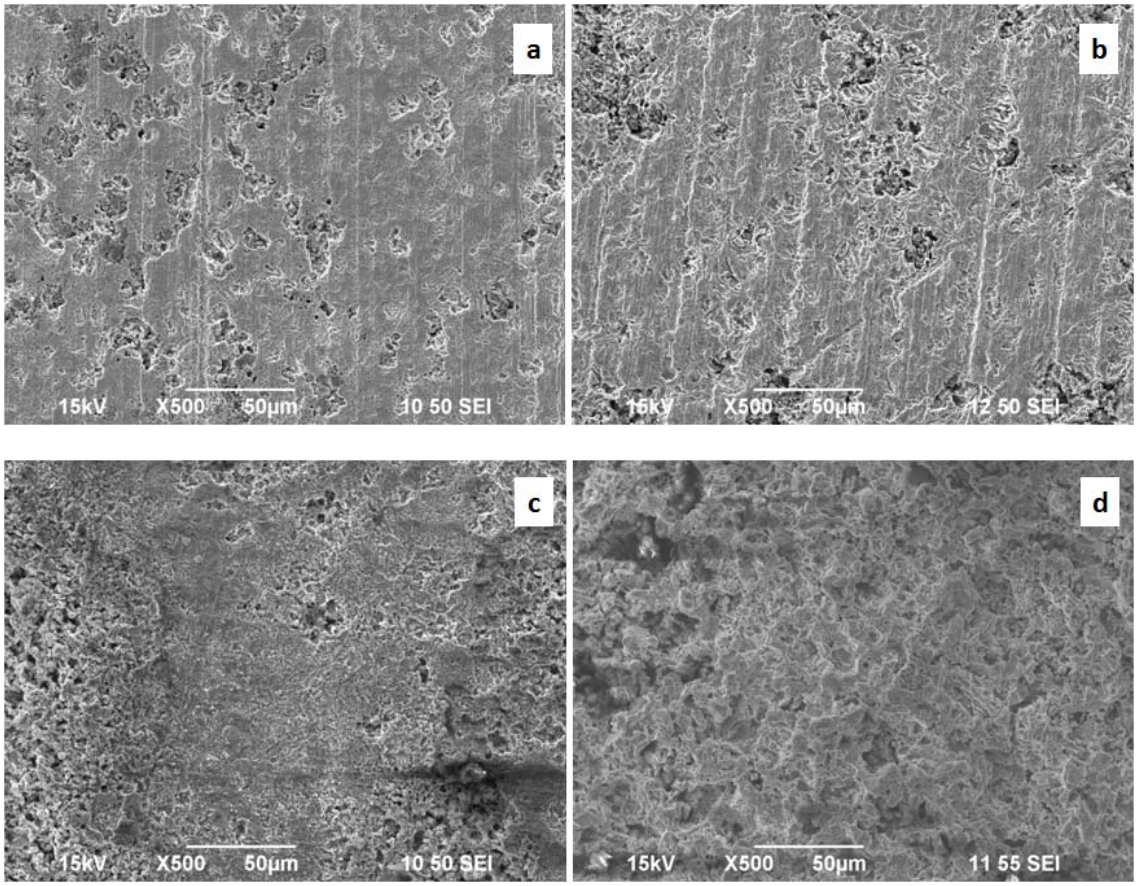


**Figure 5: SEM Images of the Corroded Surface of Samples after Cleaning: (a) 30% Water Cut, (b) 50% Water Cut, (c) 70% Water Cut and (d) 100% Water Cut**

### Experiments at 12 MPa and 65°C

Figure **6** shows the variation of metal loss with time obtained from ER measurement with different water cuts at 12 MPa and 65°C. Figure 7 compares the average corrosion rate obtained from ER, LPR and weight loss measurements at different water cuts. Similar to the results obtained at 8 MPa and 90°C, the corrosion rate increased with the increase in water cut. For 30% and 50% water cut conditions, the average corrosion rate was relatively lower than that of 70% and 100% conditions, but the corrosion rate was not negligible (e.g., 1.5 mm/y at 30% water cut and 6.0 mm/y at 50% water cut). No significant metal loss was observed by ER and weight loss measurements for the condition without water (0% water cut).

Figure 7 also shows that the corrosion rates obtained from ER, weight loss and LPR measurements all indicated very high values at 100% water cut. The difference between weight loss and LPR measurements could be attributed to the arbitrary B value (26 mV) used for calculating the corrosion rate in the electrochemical measurements.

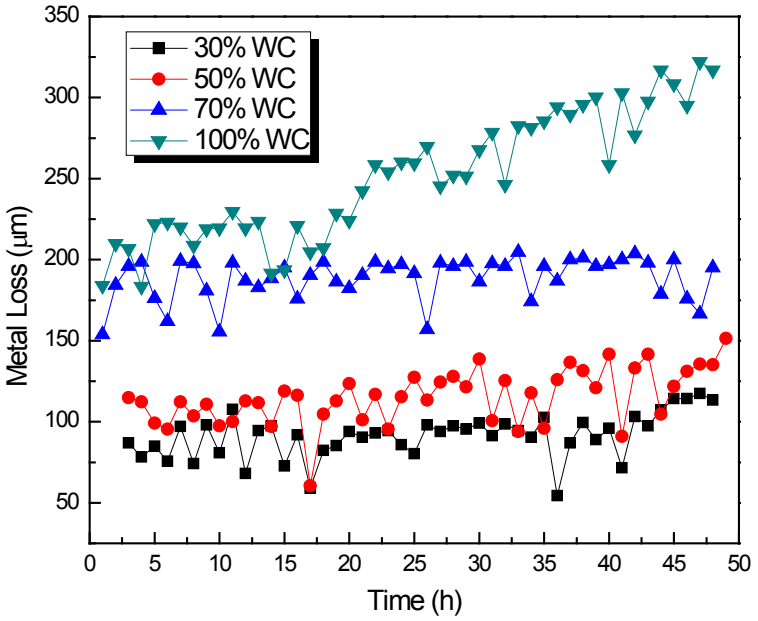


**Figure 6: Variation of Metal Loss with time Obtained from ER Measurement at Different Water Cuts (48h, 12 MPa $CO_2$, 65°C, 1000 rpm)**

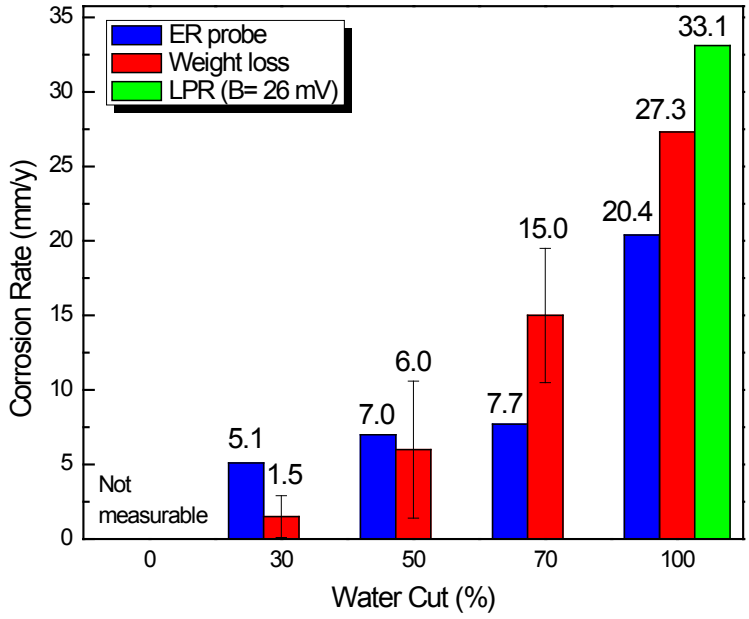


**Figure 7: Comparison of Corrosion Rates Obtained from ER and Weight Loss Measurements (average) with Different Water Cuts (48h, 12 MPa $CO_2$, 65°C, 1000 rpm)**

The SEM surface observations of the samples exposed to different water cuts are shown in Figure 8. For 0% water cut condition, no visible signs of corrosion were observed on the sample, *i.e.*, the surfaces appeared shiny and void of any type of corrosion products (Figure 8a). For 30% and 50% water cut, it can be seen that the surface morphologies were almost identical covered by $FeCO_3$ (Figure 8b and Figure 8c). For 70% and 100% water cut conditions, most of the surface was severely attacked and the corrosion product consists mainly of $Fe_3C$ and minor constituents of alloying elements from carbon steel (Figure 8d and Figure 8e).

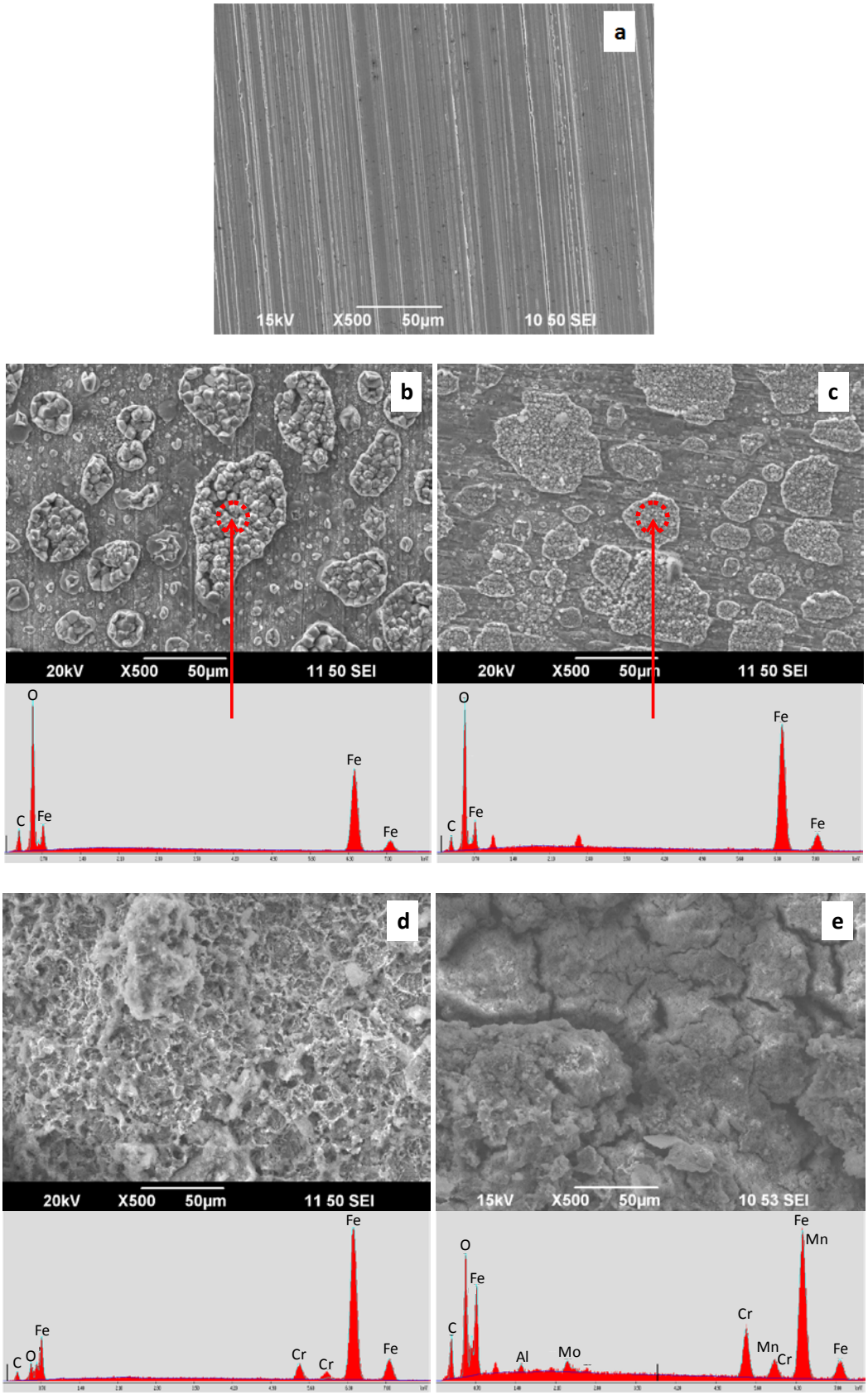


**Figure 8: SEM Images and EDS Spectra of the Corroded Surface of the Sample Exposed to: (a) 0%, (b) 30%, (c) 50%, (d) 70% and (e) 100% Water Cut (12 MPa, 65°C, 48 hours, 1000 rpm)**

Figure 9 shows the surface morphologies of samples after removing the corrosion product layer with Clarke solution. At 30% and 50% water cut conditions, the polishing marks were still visible on parts of the surface, with some scattered corrosion attack. At 70% and 100% water cut conditions, severe uniform corrosion attack was observed on the surface of the samples. For 70% water cut condition, IFM analysis (Figure 10) revealed that the depth of the penetration was around 85.5 μm, which corresponds to 15.6 mm/y. This penetration rate is similar to the weight loss corrosion rate shown in Figure 7 (15 mm/y), confirming uniform attack.

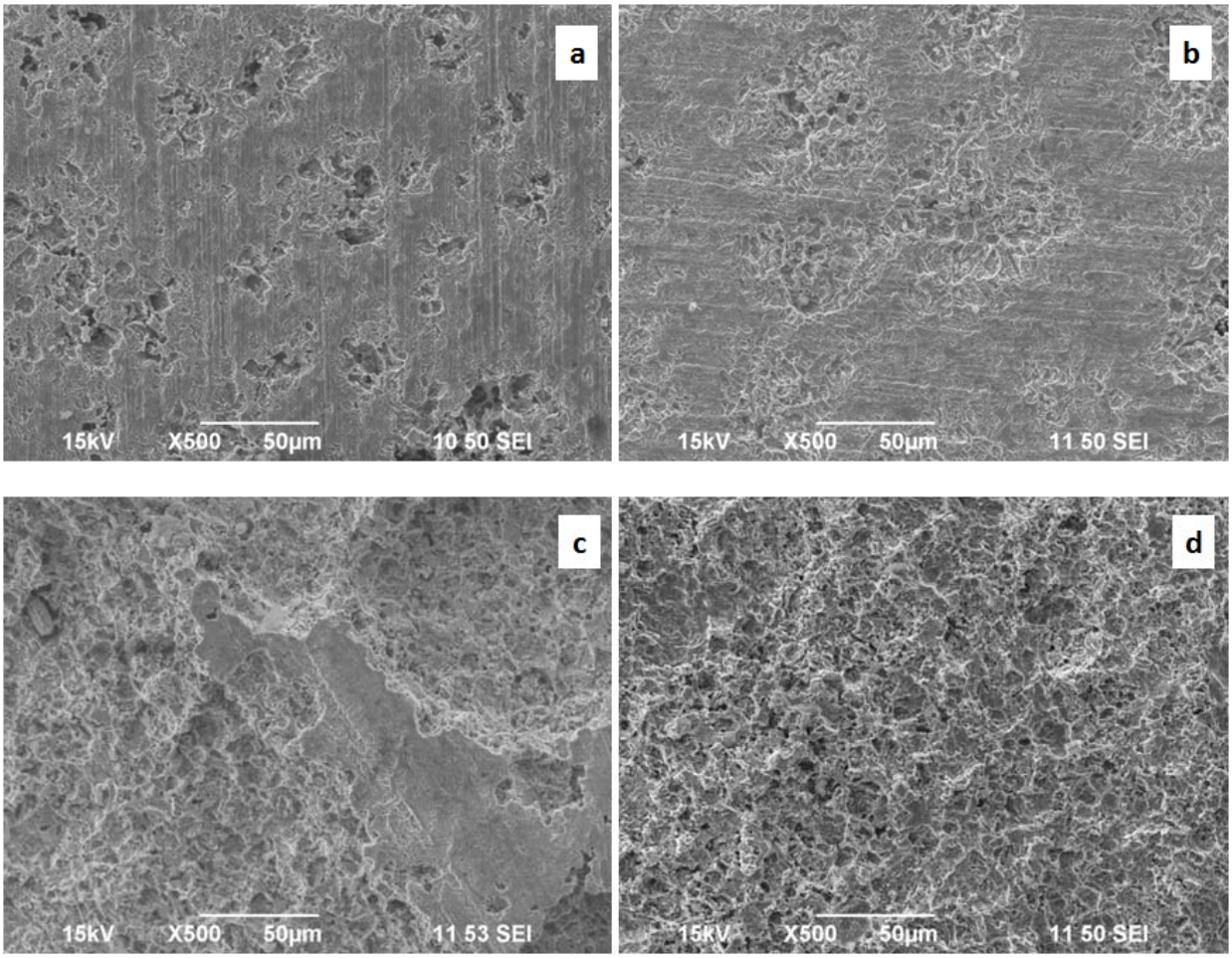


**Figure 9: SEM Images of the Corroded Surface of Samples after Cleaning: (a) 30% Water Cut, (b) 50% Water Cut, (c) 70% Water Cut and (d) 100% Water Cut**

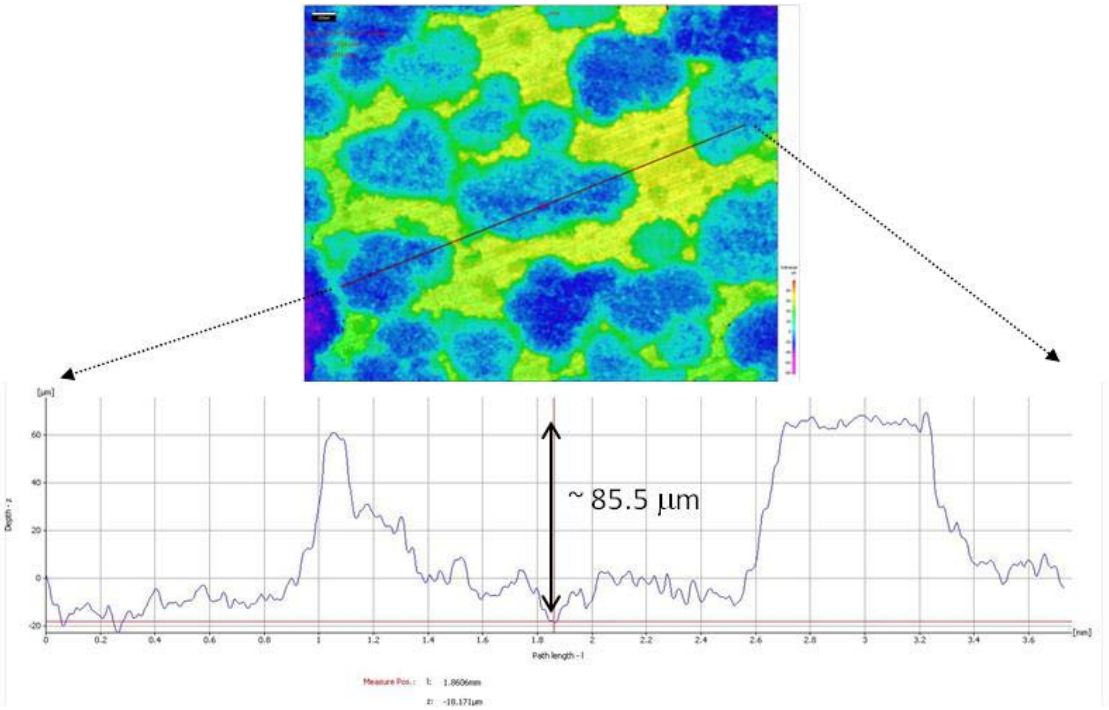


**Figure 10: Surface Profile Analysis on cleaned Surface of the Sample Exposed to 70% Water Cut Condition at 12 MPa and 65°C for 48 hours (1000 rpm)**

### Corrosion Rate Comparison between 8 MPa-90°C and 12 MPa-65°C Conditions

Figure 11 compares the corrosion rate obtained from weight loss measurements under different conditions as a function of water cut. For both conditions, the corrosion rate increased with the increase of water cut. In the mixture of crude oil and water (30 ~ 70% water cut), there is no significant difference in corrosion rate between two conditions. However, it showed higher corrosion rate in 8 MPa-90°C condition than 12 MPa-65°C due to the higher temperature which accelerates the corrosion process more than the partial pressure of $CO_2$ did.

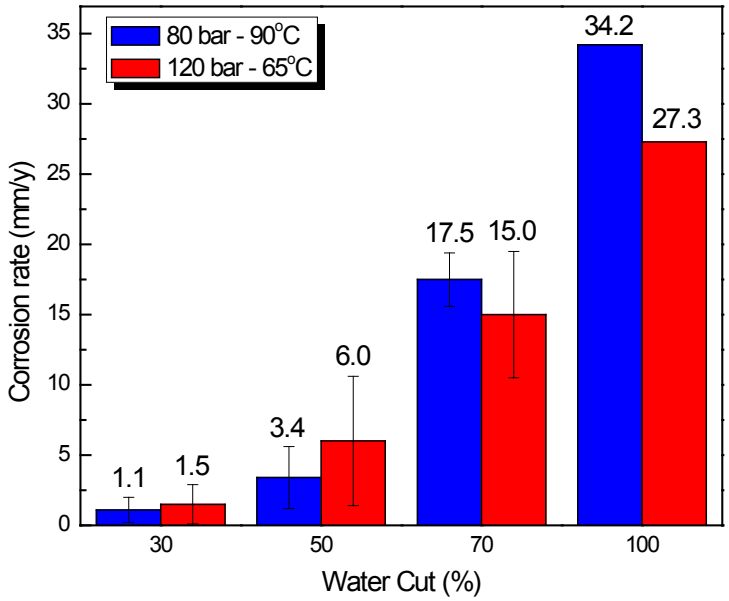


**Figure 11: Comparison of Corrosion Rates obtained from Weight Loss Measurements with different Testing Conditions and Water Cuts**

**Effect of Flow on the Corrosion Behavior of Carbon Steel with 100% Water Cut**

It is well known that the presence of flow affects $CO_2$ corrosion rate since it can enhance the transport of corrosive species towards and away from the metal surface. In addition, when the flow rate is sufficiently high, it can prevent the formation of $FeCO_3$.[12]

Figure 12 compares the corrosion rate of carbon steel obtained from weight loss measurements in a 25 wt.% NaCl solution with and without flow. As mentioned in the experimental procedures section, fast stirring (*i.e.*, 1000 rpm) was achieved using a stainless steel impeller at the bottom of the autoclave. The corrosion rates for both conditions showed higher values than those without flow. In particular, the corrosion rate at 8 MPa-90°C condition increased from 5.6 mm/y (without flow) to 34.2 mm/y (with flow).

Figure 13 shows the SEM surface images of the samples exposed to a 25 wt.% NaCl solution at 8 MPa and 90°C with / without flow. Under stagnant condition, the surface was completely covered by protective $FeCO_3$ which somewhat decreased the corrosion rate with time (Figure 13a). However, there is no indication of the presence of protective $FeCO_3$ on the surface under flowing condition (Figure 13b) and it showed severe uniform corrosion. The difference in corrosion rates between stagnant and flowing conditions can be explained by the difference in water chemistry at the steel surface. Under stagnant condition, a high concentration of ferrous ions ($Fe^{2+}$) at the steel surface and the higher surface pH would have facilitated the formation of protective $FeCO_3$ layer, leading to lower corrosion rates. However, flow and associated enhanced mass transfer would have brought more corrosive species to the steel surface and could prevent the buildup of $Fe^{2+}$ ions at the actively corroding steel surface, thereby preventing formation of a protective $FeCO_3$ on the steel and leading to higher corrosion rates.

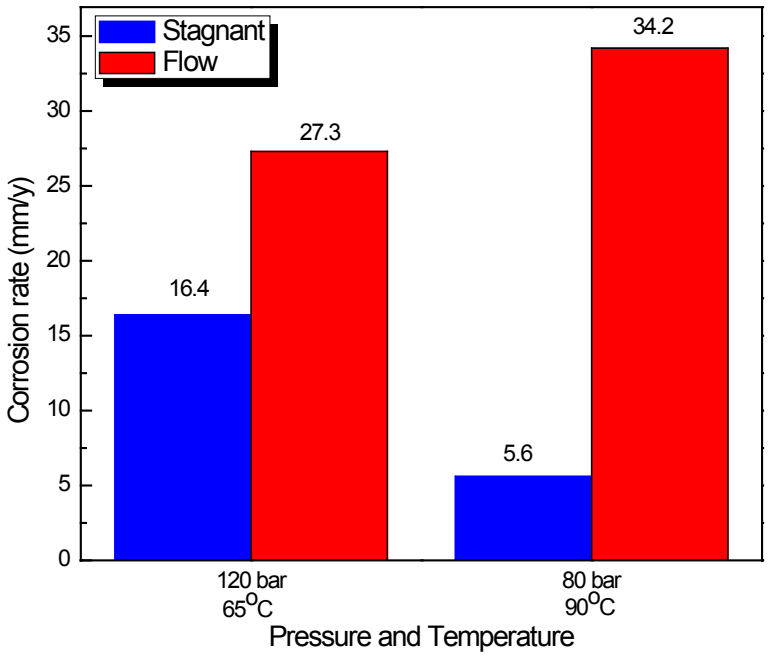


**Figure 12: Effect of Flow on the Corrosion Rate of Carbon Steel Exposed to a 25 wt.% NaCl Solution at different $CO_2$ Pressures and Temperatures**

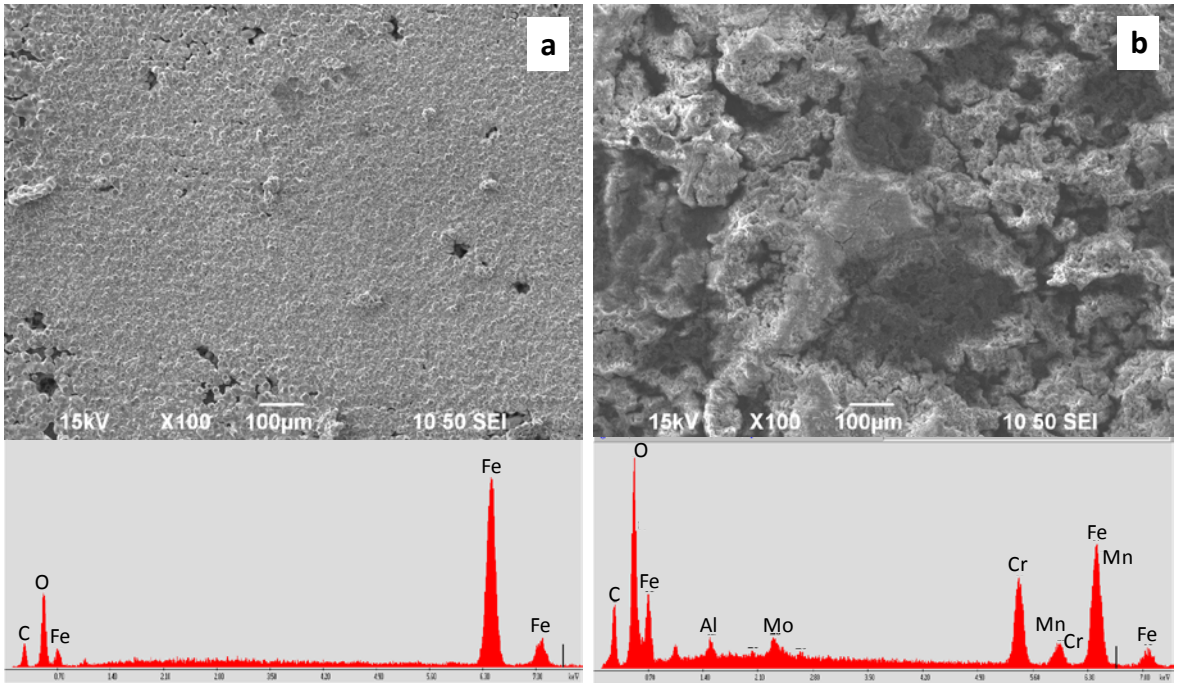


**Figure 13: SEM Images of the Sample Surfaces after Being Exposed to a 25 wt.% NaCl Solution at 8 MPa $CO_2$ and 90°C for 48 hours: (a) Stagnant, (b) Flowing (1000 rpm)**

## CONCLUSIONS

- The corrosion rate of carbon steel increased with increasing water cut under the conditions used in this study (8 MPa-90°C and 12 MPa-65°C).
- At low water cuts (30%, 50%), the sample surface was covered by some iron carbonate ($FeCO_3$) whereas iron carbide ($Fe_3C$) was predominantly presented on the steel surface at higher water cuts (70%, 100%).
- Corrosion rates ranged from high (at 30% and 50% water cut) to catastrophic (at 70% and 100% water cut).
- Flow markedly enhanced the corrosion rate and hindered the formation of a protective $FeCO_3$ layer when exposed to the aqueous phase (100% water cut).
- No localized corrosion was observed in the testing conditions.

## REFERENCES

1 Y. Zhang, X. Pang, S. Qu, X. Li, K. Gao, “Discussion of the CO2 Corrosion Mechanism between low Partial Pressure and Supercritical Condition”, Corrosion Science 59 (2012) p. 186 - 197.

2. M. F. Suhor, M. F. Mohamed, A. Muhammad Nor, M. Singer, S. Nesic, “Corrosion of Mild Steel in High CO2 Environment: Effect of the FeCO3 Layer”, CORROSION/2012, Paper No. C2012-1434, NACE, Houston, TX, 2012.

3. A. Muhammad Nor, M. F. Suhor, M. F. Mohamed, M. Singer, S. Nesic, “Corrosion of Carbon Steel in High CO2 Containing Environments - the Effect of High Flow Rate”, CORROSION/2012, Paper No. C2012-1683, NACE, Houston, TX, 2012.

4 J. A. Carew, A. Al-Sayegh, A. Al-Hashem, “The Effect of Water-Cut on the Corrosion Behaviour L80 Carbon Steel under Downhole Conditions”, CORROSION/2000, Paper No. 61, NACE, Houston, TX, 2000.

5 J. Carew, A. Al-Hashem, “$CO_2$ Corrosion of L-80 Steel in Simulated Oil Well Conditions”, CORROSION/2002, Paper No. 2299, NACE, Houston, TX, 2002.

6. Z. D. Cui, S. L. Wu, C. F. Li, S. L. Zhu, X. J. Yang, “Corrosion Behavior of Oil Tube Steels under Conditions of Multiphase Flow Saturated with Super-critical Carbon Dioxide”, Materials Letters 58 (2004) p. 1035 - 1040.

7. Electrical Resistance E/R Monitoring, available from: **http://www.alspi.com/erintro.htm**

8. Gerald S. Frankel, “Electrochemical Techniques in Corrosion: Status, Limitations, and Needs”, Journal of ASTM, Vol. 5, No. 2, Paper ID JAI101241.

9. Y. S. Choi, F. Farelas, S. Nesic, A.A.O. Magalhães, C. de Azevedo Andrade, “Corrosion Behavior of Deep Water Oil Production Tubing Material under Supercritical $CO_2$ Environment: Part I. Effect of Pressure and Temperature”, to be presented in NACE 2013, Orlando Florida, NACE, Houston, TX, 2013.

10. J. Crolet, N. Thevenot, S. Nesic, “Role of Conductive Corrosion Products in the Protectiveness of Corrosion Layers”, Corrosion 54 (1998) p. 194.

11. ASTM Standard G1-03, “Standard Practice for Preparing Cleaning and Evaluating Corrosion Test Specimens”, Annual Book of ASTM Standards, vol. 03. 02 (West Conshohocken, PA: ASTM International, 2003) .

12. S. Nesic, “Key Issues Related to Modelling of Internal Corrosion of Oil and gas Pipelines – A Review”, Corrosion Science 49 (2007) p. 4308 - 43338.